Marine Geology 381 (2016) 42–53

Contents lists available at ScienceDirect

Marine Geology

journal homepage: www.elsevier.com/locate/margo

Decoupling processes and scales of shoreline morphodynamics

Cheryl J. Hapke [a,*], Nathaniel G. Plant [a], Rachel.E. Henderson [a], William C. Schwab [b], Timothy R. Nelson [a]

[a] U.S. Geological Survey, St. Petersburg Coastal and Marine Science Center, 600 4th St South, St Petersburg, FL 33701, United States
[b] U.S. Geological Survey, Woods Hole Coastal and Marine Science Center, 384 Woods Hole Rd, Woods Hole, MA 02543, United States

ARTICLE INFO

Article history:
Received 27 March 2016
Received in revised form 6 August 2016
Accepted 22 August 2016
Available online 24 August 2016

Keywords:
Shoreline change
Coastal evolution
Storm response
Empirical orthogonal function
Fire Island

ABSTRACT

Behavior of coastal systems on time scales ranging from single storm events to years and decades is controlled by both small-scale sediment transport processes and large-scale geologic, oceanographic, and morphologic processes. Improved understanding of coastal behavior at multiple time scales is required for refining models that predict potential erosion hazards and for coastal management planning and decision-making. Here we investigate the primary controls on shoreline response along a geologically-variable barrier island on time scales resolving extreme storms and decadal variations over a period of nearly one century. An empirical orthogonal function analysis is applied to a time series of shoreline positions at Fire Island, NY to identify patterns of shoreline variance along the length of the island. We establish that there are separable patterns of shoreline behavior that represent response to oceanographic forcing as well as patterns that are not explained by this forcing. The dominant shoreline behavior occurs over large length scales in the form of alternating episodes of shoreline retreat and advance, presumably in response to storms cycles. Two secondary responses include long-term response that is correlated to known geologic variations of the island and the other reflects geomorphic patterns with medium length scale. Our study also includes the response to Hurricane Sandy and a period of post-storm recovery. It was expected that the impacts from Hurricane Sandy would disrupt long-term trends and spatial patterns. We found that the response to Sandy at Fire Island is not notable or distinguishable from several other large storms of the prior decade.
Published by Elsevier B.V.

1. Introduction

In the aftermath of extreme storm events there tends to be an increased societal focus on understanding the processes that control variations in coastal response, such as shoreline erosion and recovery. Such knowledge can be used for the development and refinement of models that predict future coastal behavior, and provides fundamental information needed to understand coastal vulnerability and resiliency. It is important to consider the relative roles of the various drivers of coastal change and the time scales of their influence when developing predictive models of coastal evolution in geologically and oceanographically complex coastal systems such as barrier islands.

Hydrodynamics are a primary driver of coastal change. Water levels and currents associated with waves, surge and tides interact with beach and bar morphology and associated sedimentary deposits to drive beach and shoreline response during single storm events and stormy periods (Lippmann and Holman, 1990; Plant et al., 1999; Sallenger, 2000; Stockdon et al., 2006; Wright and Short, 1984) and over longer timescales (e.g., Yates et al., 2009). The alongshore variability of wave energy reaching the coast can be influenced by the orientation of the coast, the bathymetry of the adjacent inner shelf and shoreface, and the morphology of the nearshore bar and surf zone. Morphodynamic response of a beach during storms is driven by hydrodynamic processes, but other factors, such as alongshore variations in beach and shoreface slope, island elevation, and sediment availability may also impact short-term beach response (Tătui et al., 2014; Wright and Short, 1984).

Longer-term behavior (years to decades) of the shoreline is the result of hydrodynamic and morphodynamic processes acting over multiple stormy and intervening calm periods during which the advanced or retreated state of the shoreline may be increasingly influenced by sediment supply and geology (Houser et al., 2008; Morton et al., 2007; Viles and Goudie, 2003; Woodroffe, 2003). Determining the relationship between shoreline processes and the response of the shoreline over a continuum of time scales requires data of sufficient temporal and spatial resolution and extent to resolve these scales (Stive et al., 2002).

Shoreline data capable of resolving storm events, annual and multi-decadal response are uncommon, and as a result few studies have examined shoreline behavior over a broad range of time scales. And while oceanographic forcing parameters (e.g., offshore wave height and direction) can be evaluated over long time periods using data from wave buoys and tide gauges, or from modeled hindcast results (U.S. Army Corps of Engineers Wave Information Studies, for example). However, hydrodynamic processes alone are not sufficient to explain all

* Corresponding author.
E-mail address: chapke@usgs.gov (C.J. Hapke).

http://dx.doi.org/10.1016/j.margeo.2016.08.008
0025-3227/Published by Elsevier B.V.

shoreline variability over multiple time and space scales. Internal characteristics (e.g., framework geology and geomorphology) of barrier island systems exert control on both the long-term and/or short-term responses to the hydrodynamics.

Studies abound in the literature that describe the importance of framework geology on barrier island coastal evolution and response. The foundational studies of Belknap and Kraft (1985) and Riggs et al. (1995) related characteristics of the underlying stratigraphy of the inner continental shelf in North Carolina, including stratigraphic variations and sediment availability, to barrier island evolution over long temporal scales. Schwab et al. (2000, 2013) extended the North Carolina studies to examine the relationship between stratigraphic and lithologic variations in the pre-Holocene and Holocene deposits of the inner continental shelf off Fire Island, New York, and centennial scales of shoreline change. McNinch (2004), Miselis and McNinch (2006) and Schupp et al. (2006) built on the previous works but focused on smaller scales of framework geology and shoreline change. The studies examined the occurrence of paleochannels and deposits within the shoreface along a single barrier island and found a relationship between the patterns of decadal shoreline change and variable sediment availability, with shoreline erosion in areas dominated by paleochannels.

Hapke et al. (2010, 2011b) established the relationship between shoreline change on a variety of time scales (decades to century) and the modern morphology and framework geology of the inner shelf at Fire Island. Persistent shoreline undulations were shown to occur coincidently with the section of the island where a shoreface-attached ridge system extends into the very nearshore (~3–4 m water depth) and appears to influence hydrodynamic processes. Further, Lentz et al. (2013) spatially correlated decadal beach-dune morphology and response, including zones of persistent overwash, to variations in storm wave water levels that are related to bathymetric variations on the inner shelf. Thus, the framework geology, which controls the bathymetric variability is shown to be linked to island response on storm to decadal scales.

The above introduction is by no means a complete overview of the research that has established linkage between framework geology and coastal response. Such an effort is outside the scope of this paper. However, the examples and references therein provide the foundational knowledge that framework geology has an important and demonstrable influence on rates and trends of shoreline change on a variety of time scales. A question that remains is what is the relative importance of storm processes versus geological control on storm response and multi-decadal evolution of barrier islands?

In this paper, we utilize a statistical approach to examine spatial and temporal variations in the morphologic evolution and response of the shoreline at Fire Island, NY, and relate the behaviors to the influences of geology and storm processes. In addition, we take advantage of an enhanced temporal resolution of our shoreline data to capture the short-term response of a recent extreme storm event.

We hypothesize that there are separable patterns in shoreline response that can be utilized to examine the role of oceanographic forcing of storms of varying sizes versus geologic control. There may be feedback between the different components that alter how the system responds if there are large shifts in morphology or geology. For instance, large storms could change the distribution of sediment supply and alter subsequent patterns of short-term and long-term response. Hurricane Sandy (landfall on Oct. 29, 2012, near Atlantic City, NJ) is an event that we investigate to explore whether extreme storms alter the stability of the island, altering the relationship between geology and long and short time-scale behavior.

Fire Island is an ideal locale for examining this relationship due to the complex, but well-documented framework geology, distribution of sand deposits on the inner shelf, and variable bathymetry and island topography (Hapke et al., 2011b; Leatherman, 1985; Lentz and Hapke, 2011; Lentz et al., 2013; Schwab et al., 2000, 2013, 2014). We utilize an extensive database of shoreline positions that extends over a time period of 81 years to examine the morphodynamics of the shoreline over multiple time scales and assess the dominant controls on the spatial variations and temporal trends. The variance in the time series is analyzed using empirical orthogonal functions (EOF) to statistically evaluate temporal trends and spatial patterns that dominate the shoreline behavior. This approach allows us to decompose the complex time series to isolate the relative importance of the factors controlling shoreline behavior and the scales over which they have influence. We then describe the different modes, attribute them to oceanographic, geologic, or feedback processes, and identify what processes control shoreline variability at different spatial and temporal scales.

2. Oceanographic and geologic setting

Fire Island is part of the barrier island system that flanks the south shore of Long Island, New York (Fig. 1). The island is oriented east-northeast and extends for 50-km from Fire Island Inlet in the west to Moriches Inlet in the east. Both inlets are stabilized with jetties and periodically dredged to maintain navigation channels. The Fire Island coastal system is wave-dominated, microtidal, with a tidal range of 1.3 m (NOAA, 2014). Sediment transported along the shore of Fire Island is primarily from east to west, driven by the predominant wave approach out of the southeast (Leatherman, 1985). The ocean coastline of Fire Island is modified by storms and subsequent recovery. The most common severe storms are extratropical (nor'easter) systems that occur seasonally, typically from November through April. Nor'easters tend to have durations extending over multiple tidal cycles, generally 2–5 days. In contrast, hurricanes directly impact Fire Island less frequently and in general are faster moving systems, with impacts occurring over one or two tidal cycles, typically lasting <24 h (Birchler et al., 2015). Historic storms of note can be identified from reports of widespread erosion, overwash, breaching, and infrastructure damage along this coastline. Examples of such storms include the 1938 Hurricane, the 1962 Ash Wednesday storm, a series of powerful nor'easters in 1991, 1992 and 1993, and Hurricane Sandy in 2012. Significant wave heights during Hurricane Sandy reached the highest levels on record, 9.6 m (from NDBC wave buoy #44025) (Hapke et al., 2013).

Distinct variations in the morphology of the inner continental shelf and modern sediment distribution patterns offshore of Fire Island (Schwab et al., 2013, 2014) allow the system to be divided into three distinct geologic zones. Remnants of a Pleistocene glaciofluvial outwash lobe define a submerged headland offshore of central Fire Island (Fig. 1). The zone is more gently sloping than the adjacent areas and contains thicker deposits of sediments. To the east of the submerged headland, relatively older Pleistocene outwash is exposed over much of the inner continental shelf; little modern sediment exists in this zone (Schwab et al., 2000, 2013, 2014). The morphology of the inner continental shelf offshore of western Fire Island is dominated by a field of shoreface-attached sand ridges that migrate in a westerly direction (Duane et al., 1972; Schwab et al., 2013, 2014).

The morphologic behavior and storm response of the island is relatively well documented and both shoreline and profile morphodynamics have been related to the regional variations in inner shelf geology (Hapke et al., 2013; Leatherman, 1985; Lentz and Hapke, 2011; Lentz et al., 2013; Schwab et al., 2013). The historical record of shoreline change along Fire Island can be separated into three zones which correspond to the three geologic zones identified on the inner continental shelf. Schwab et al. (2013) noted that the rates of change are highly variable along the coast with erosion along the eastern segment of the island (-0.72 ± 0.18 m/year), modest shoreline accretion in the central segment of the island (0.38 ± 0.07 m/year) and mixed erosion and accretion along the western segment (-0.12 ± 0.14). In this paper we refer to the different zones as the western, central and eastern geologic zones (WGZ, CGZ, and EGZ).

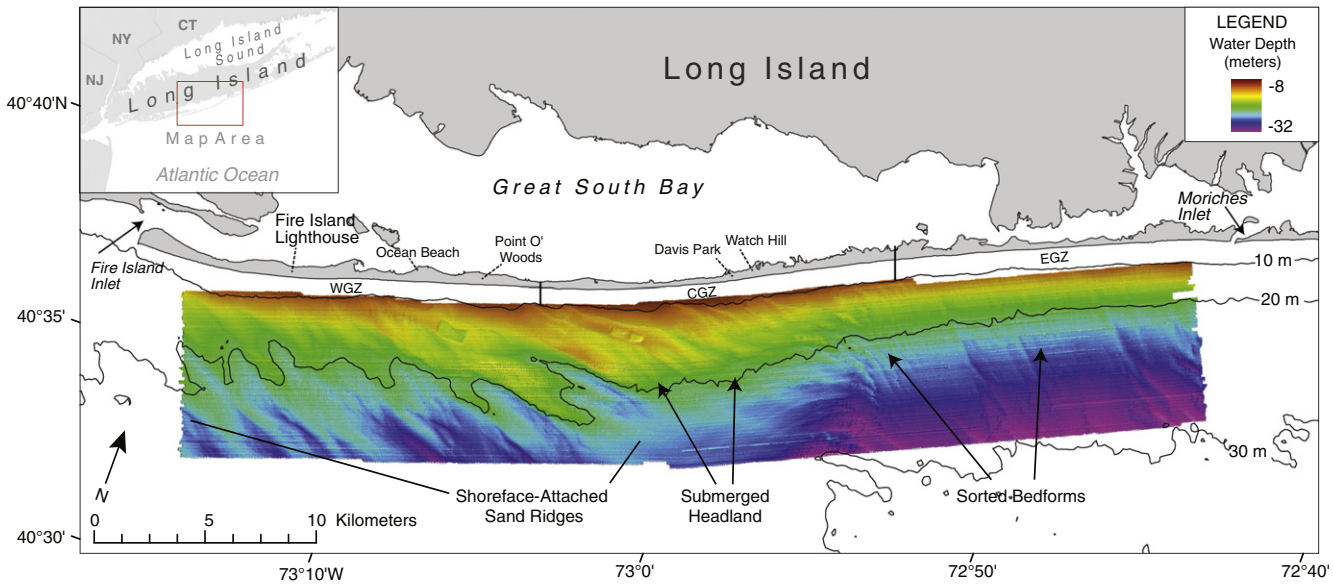

Fig. 1. Location map of Fire Island showing inner shelf geology (modified from Schwab et al., 2013), bathymetry, and the west (WGZ), central (CGZ) and east (EGZ) geologic zones.

3. Methods

3.1. Shorelines and time series analysis

Shorelines incorporated into this analysis are largely derived from previous data compilations (Table 1) (Hapke et al., 2011a; Himmelstoss et al., 2010; Lentz et al., 2013; Schwab et al., 2013). For this study, the extensive historical shoreline database is supplemented with new data collected immediately prior to and after Hurricane Sandy (October–November 2012) and over a period of fifteen months after Sandy to document recovery (Henderson et al., 2015). The post-Sandy shorelines are derived from field data acquired using DGPS survey lines collected on the beach face and extracting the MHW contour from an interpolation of the survey data (Hapke et al., 2013). Older shorelines (pre-1997) are based on interpretations of high-water lines (HWL) from historical maps and wet-dry lines (WDL) identified in aerial photographs. More recent shorelines (1997 to 2014) are mean high water (MHW) contours derived from lidar elevation datasets or ground surveys. Estimates of shoreline positional uncertainty contained in this database (Table 1) were derived using methods established by Himmelstoss et al. (2010) and Hapke et al. (2011a) by assessing the errors associated with the data sources, collection, extraction or digitization of the shorelines, and summing the error terms in quadrature. This uncertainty ranges from 1 to 5 m.

Shoreline change rates using twenty-three shorelines from previous analyses (Hapke et al., 2010; Schwab et al., 2013) and five additional shorelines are used to extend the long-term record and examine the impact and recovery from Hurricane Sandy (Table 1). The shoreline database contains numerous historical shorelines for years in which storms occurred but none of the data were collected specifically to resolve storm events and subsequent recovery. The additional data from 2012 to 2014 allows for a more detailed examination of an extreme storm event (Hurricane Sandy) at Fire Island.

A regular time-series array is developed from mean-removed shorelines and allows visualization of persistent trends, temporal oscillations and spatial variations of the shoreline. The temporal mean shoreline position is calculated using the time series of shorelines (1933–2014). This value is then subtracted from each observed shoreline position such that positive values in Fig. 2 represent shorelines that are seaward of the mean and negative values are landward of the mean. The array is created using a linear Delauney triangulation to interpolate between individual dates and locations to create a Triangulated Irregular Network

Table 1
Overview of shoreline data and uncertainty statistics.

Shoreline dates	Number of shorelines	Uncertainty (m)	Shoreline proxy	Shoreline originator	Data source	Data originator
7/01/1933, 7/01/1938[a]	2	10.8	HWL	USGS[b]	T-Sheet, aerial photography	NY Sea Grant
7/01/1962, 7/01/1979[a]	2	5.1	MHW, WDL	USGS[b]	Aerial photography	NY Sea Grant, UMD
3/23/1969, 3/28/1969	1	5.1	WDL	USGS	Aerial photography	URI/NPS
7/01/1983, 7/01/1988	2	3.2	WDL	USGS[b]	Aerial photography	NY Sea Grant
8/11/1993, 9/11/1994, 8/21/1995, 8/23/1996, 9/22/1997, 9/11/2001, 10/16/2006	7	3.2	HWL	USGS/NPS[c]	Field survey	NPS/USGS
12/03/1998, 10/21/1999, 9/30/2000, 10/08/2002, 4/25/2005, 4/30/2007, 7/09/2009, 8/16 & 8/29/2010, 8/31/2011, 5/07/2012, 11/05/2012	11	2.0	MHW[d]	USGS	Lidar	USGS/NPS/NOAA/NASA
3/13/2013, 9/19/2013, 1/30/2014	3	1.2–5.5	MHW[d]	USGS	Field survey	USGS

HWL - high water line; WDL - wet dry line; MHW - mean high water.
[a] 07/01/YEAR is a default date used when the actual survey date is unknown, or spanned over multiple dates. It is assumed that 1938 and 1962 are post-hurricane aerial surveys.
[b] http://pubs.usgs.gov/of/2010/1119/.
[c] https://irma.nps.gov/App/Reference/Profile/2174499.
[d] The operational MHW for Fire Island, NY is 0.46 m NAVD88.

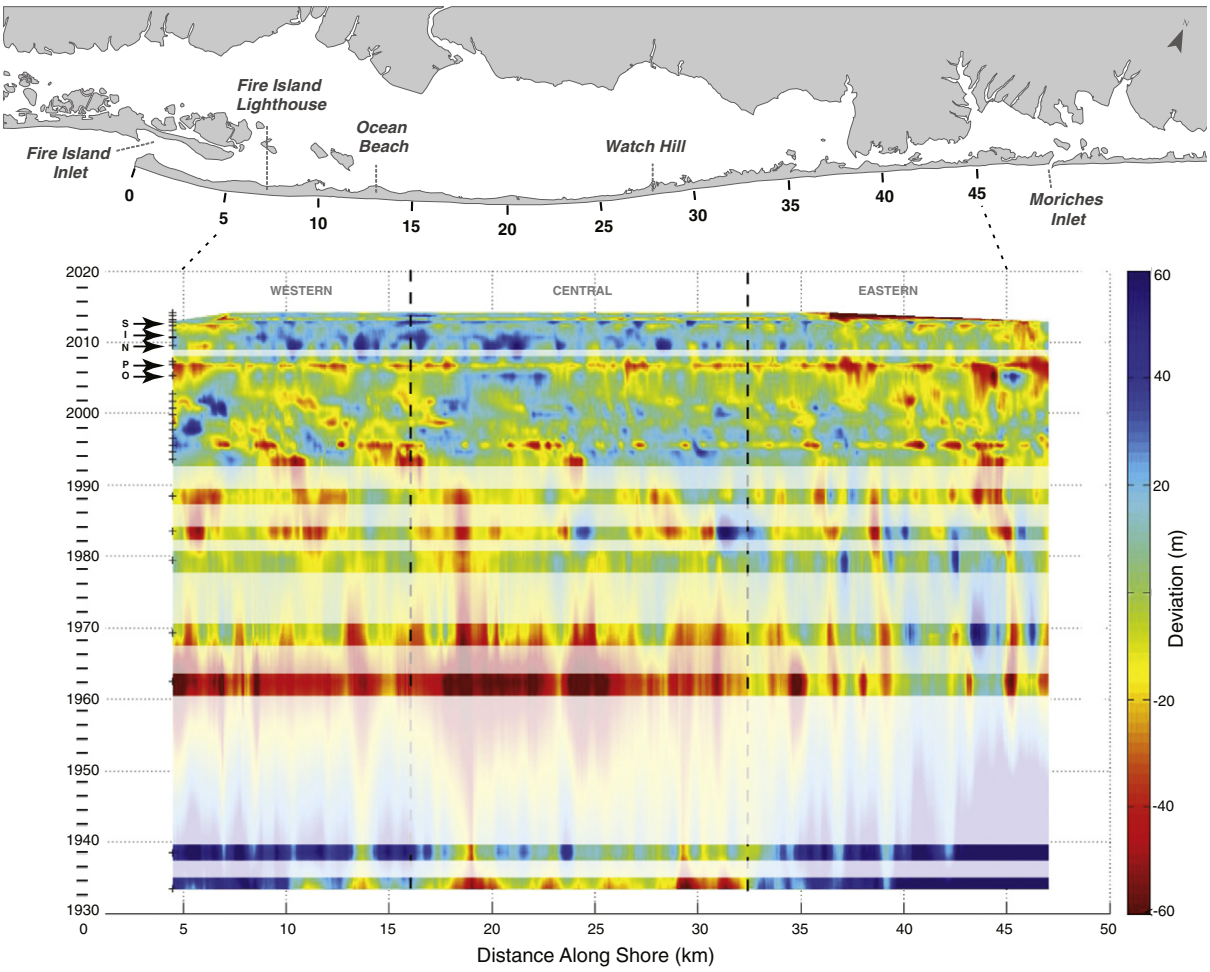

Fig. 2. Time series of mean-removed shoreline position. The gray boxes are data gaps over which residuals are averaged over long time periods and have high levels of uncertainty. Recent significant storms are represented by the arrows and letters: O = Oct. 2005 nor'easter; P = 2007 Patriot's Day nor'easter; N = 2009 Nor'Ida storm; I = 2011 Hurricane Irene; S = 2012 Hurricane Sandy. The 3 geologic zones are also demarcated.

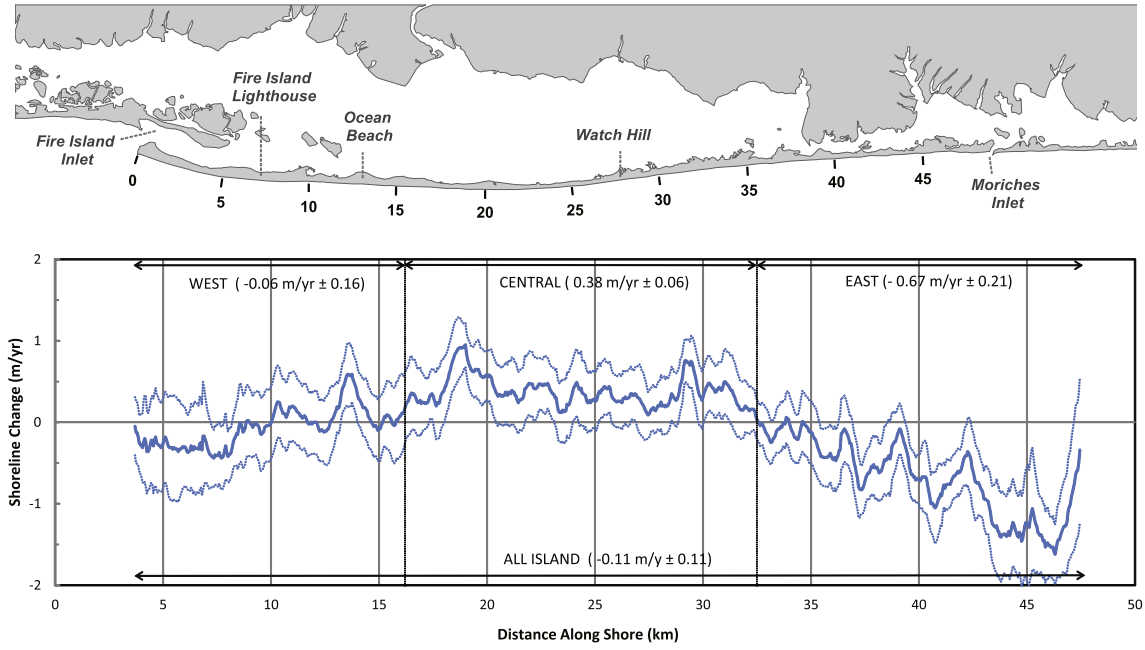

Fig. 3. Long-term linear regression plot of shoreline change rates, with the 95% confidence band (dashed line) around the average rate (solid line). The vertical dashed lines show the divisions of the western, central and eastern geologic zones.

(TIN)·Where there are large temporal gaps in the sampling record (for example between 1940 and 1960 in Fig. 2), the interpolated grid cell values have a higher degree of uncertainty due to aliasing. However, persistent variations are still clearly resolved. For example, the zone of erosion in the area 18–20 km alongshore (Fig. 2) is persistent over long periods of time (1933 to 1989) and the interpolated grid provides a visual representation of the spatial continuity of that behavior through time.

Shoreline change rates are calculated at 50 m intervals using the Digital Shoreline Analysis System (DSAS; Thieler et al., 2009) to generate linear regression rates and other change statistics (Fig. 3). The analysis does not include the very eastern and western portions of the island, 2 and 4 km from the inlets, respectively, in order to exclude the large signals of accretion associated with the construction of the inlet jetties and associated inlet bypassing in the case of Moriches Inlet.

The uncertainties for the linear regression rates are calculated following the method outlined in Hapke et al. (2011a) and Hapke et al. (2013). The approach uses a spatially-lagged autocorrelation (Garrett and Toulany, 1981) to determine the number of independent transects in the area along which rates are being averaged. A quadrature average of the 95% confidence interval (Taylor, 1997) is then determined using a reduced number of independent transects.

3.2. EOF (empirical orthogonal function) analysis

We use empirical orthogonal function analysis (EOF) as a tool for identifying coherent spatial and temporal variability. EOF has been used in a variety of applications in coastal systems. Most have applied the technique to evaluate dominant modes of variability in the cross-shore direction (Houser et al., 2008; Wijnberg and Terwindt, 1995; Winant et al., 1975; Yates et al., 2011) while some researchers have used EOF to assess trends and patterns in alongshore variability in shoreline position (Dick and Dalrymple, 1984; Munoz-Perez et al., 2001; Miller and Dean, 2007). In this study, EOF analysis is used to separate the spatial and temporal patterns of the mean-removed shoreline position data. The EOF analysis solves for independent modes that can be used to reconstruct the input data as

$$X(y,t) \sim \sum_{m=1}^{M} A_m(t)\,F_m(y) \quad (1)$$

where X indicates the mean-removed shoreline position data, and y and t indicate alongshore position and time, A_m are temporal modes, F_m are spatial modes, and the summation is over all possible modes, M, which equals the number of spatial locations included in the analysis ($M = 839$). To compute the EOF modes, spatial and temporal data gaps were filled prior to EOF analysis via interpolation that used a smoothing filter (Plant et al., 2002) with 250-m half-width in the alongshore direction and 1-month half-width in time. The temporal smoothing removed very rapid fluctuations in cases where there were frequent surveys that sampled individual storm response and recovery. Spatial gaps wider than 250 m were treated as missing data following the approach of Davis (1976), which finds weighted values for the EOF amplitudes (A_m) when data are missing, reducing sample bias at times when the data are not complete. We define the EOF spatial modes (F_m) such that they are normalized to have unit variance and the temporal modes (A_m) carry the actual variance explained by each mode. The modes are sorted such that those with the most variance are presented first and, as we will show, the first few modes are the only ones that contain relevant signals and the later modes are attributed to noise. Additionally, because the modes are, by definition, independent of each other, we can interpret each one individually and attempt to assign different physical process or geological significance to each one, independent of the other modes.

3.3. Wave record analysis

To examine whether temporal variations in the EOF modes can be related to hydrodynamic forcing as opposed to geologic processes, we analyzed available wave and water level records and compared them to the EOF. We used Wave Watch 3 (WW3) data from 1979 to 2015, which consist of reanalysis hindcast data between January 1979 and January 2005. Historical observed data were used between February 2005 and January 2015 (http://polar.ncep.noaa.gov/waves/). The wave time series is taken from a WW3 grid point offshore of Central Fire Island (40.6°N and 72.93°W). Hourly water level observations from 1933 to 2015 were also obtained from the NOAA tidal station 8531680 located at Sandy Hook, NJ. Table 2 shows the mean and standard deviation of the wave characteristics averaged over 5 year periods.

4. Results

4.1. Shoreline morphodynamics

The regular time series array of mean-removed residual shoreline position is shown in Fig. 2 and shows 81 years of shoreline response. The temporal pattern of change includes advanced (shoreline seaward of the mean) or retreated (shoreline landward of the mean) states that persists for a period of time and then the patterns reverse. For example, the shoreline is in an advanced state in the pre-1950 period (Fig. 2). From 1950 to 1970, the shoreline is in a dominantly retreated phase. Beginning about 1970, the phase shifts back to an advanced phase for approximately 10 years, and then retreats again beginning about 1980. The system appears to fall out of this oscillatory phase behavior from the 1990s to ~2005. Shorter duration cycles of shoreline advance and retreat are better resolved in the shoreline record in the near-term (Table 1) when the data are sampled more frequently. Prior to the 1990s, the sample frequency of the data is not sufficient to resolve smaller scale variations that would have occurred on time scales of years, for instance during stormy periods versus non-stormy periods.

In addition to oscillations of shoreline position through time, there are also alongshore zones of retreat or advancement that are spatially persistent over long time periods (Fig. 3).The results of the linear regression analysis, conducted on the 81-year shoreline position dataset (Fig. 3), expand on those presented by Schwab et al. (2013), with an along-island average of -0.11 ± 0.11 m/year, which is not significantly different from zero. The rates are highly variable alongshore, but the long-term trends are distinct within the three geologic zones of Fire Island. EGZ shows relatively high rates of erosion (-0.67 ± 0.21 m/year).

Table 2
Mean and standard deviation over a 5 year period for wave height, wave period, wave direction or propagation, and surge.

Years		Wave height (m)		Wave period (s)		Wave direction (deg)		Surge (m)	
		μ	σ	μ	σ	μ	σ	μ	σ
1935	1939							−0.21	0.17
1940	1944							−0.21	0.18
1945	1949							−0.17	0.17
1950	1954							−0.14	0.18
1955	1959							−0.11	0.18
1960	1964							−0.11	0.18
1965	1969							−0.09	0.18
1970	1974							−0.04	0.18
1975	1979							−0.07	0.18
1980	1984	1.09	0.61	7.30	2.68	−32.41	49.98	−0.03	0.17
1985	1989	1.07	0.58	6.89	2.58	−27.86	49.14	−0.03	0.16
1990	1994	1.10	0.61	7.07	2.62	−29.29	50.47	−0.02	0.18
1995	1999	1.12	0.63	7.02	2.63	−25.35	49.72	0.04	0.17
2000	2004	1.10	0.57	6.75	2.47	−22.87	50.21	0.03	0.16
2005	2009	1.07	0.59	7.02	2.53	−25.70	52.28	0.08	0.18
2010	2014	1.03	0.58	7.26	2.63	−26.16	53.25	0.12	0.17
Complete		1.08	0.6	7.06	2.61	−27.15	50.61	−0.06	0.20

CGZ is characterized by an accretional trend (0.38 ± 0.06), and rates of change in WGZ are highly variable along the coast with an average of -0.06 ± 0.16 m/year (no significant change).

4.2. Empirical orthogonal function analysis

In the EOF analysis for the full time series (1933–2014, Fig. 4), 67% of the alongshore position variability is described by three EOF modes, herein referred to as EOF1, EOF2 and EOF3, explaining 33%, 19%, and 15% of the variance, respectively. EOF1 has the same sign (negative) along the length of the island, and, thus, represents shoreline changes that are in phase with each other over the entire coast (Fig. 4A). This in-phase behavior can represent shoreline response typical of cross-shore seasonal and storm behavior wherein the entire shoreline advances or retreats in response to alongshore uniform driving forces (Miller and Dean, 2007). EOF1 contains both short-scale and larger-scale spatial variability indicating differences in the amplitude of the responses. For instance, at the far western end of the island, the amplitude is nearly zero indicating that this mode describes very little of the variance there. The amplitude increases within the rest of WGZ, is somewhat smaller in CGZ, and increases again in EGZ. There are slight negative trends in the mode from the central area of the island towards either end with the exception of the near-zero west end of the island next to Fire Island Inlet.

The temporal eigenfunction associated with EOF1 indicates that there are strong oscillations, which are consistent with storm response and recovery as the shoreline moves landward and seaward across the entire region (Fig. 4B). The sparse sampling prior to the 1980s might suggest a trend between the 2nd and 3rd observations where the temporal function experiences a large change (and change in sign). However, it is likely that there were many oscillations in the temporal response that were not resolved. After the early 1990s, the improved resolution of the data shows that the amplitude variations are very noisy and oscillate around zero through the remainder of the time series.

The EOF2 mode accounts for 19% of the variance in the time series. Spatial variability associated with this mode includes distinct differences in behavior of the island (Fig. 4C). In the WGZ, there is alongshore variation with a characteristic length scale of approximately 6 km. There is a strong trend from high to low variance between EGZ to CGZ with a phase reversal in the transition area between the two zones. The temporal coefficient of EOF2 shows that the distinct spatial variation of the long-term shoreline behavior between zones is dominant early in the time series (~pre-1970), and vanishes around 2000, and has an opposite sign thereafter (Fig. 4D). This behavior corresponds to a large-scale change in the shoreline angle as the east end of the island retreats landward, the middle accretes, and the west is variable but stable, as documented by the linear regression shoreline change patterns (Fig. 3).

EOF3 describes 15% of the variance in the shoreline record. Spatial patterns include large amplitude oscillations on the western half of the island with wave lengths of 6–7 km (Fig. 4E). The length scale of the oscillations in EOF3 is similar to the oscillations present in EOF2, but the location of the peaks of the oscillations is spatially shifted, a requirement since the different modes are uncorrelated. The temporal coefficient shows little coherent change until the mid-1990s (Fig. 4F) when there is a progressive change in amplitude (it becomes negative), after which there is a reversal in the amplitude (trending towards positive) until stabilizing during the more recent dates (~post-2002) with a slight positive value. On the western half of Fire Island, this indicates a change in the phase of the rhythmic features such that the locations where the shoreline had been in an advancing state have reversed to a retreating state. The same is true for the eastern half of the island, although the oscillations do not exhibit a systematic length-scaling as

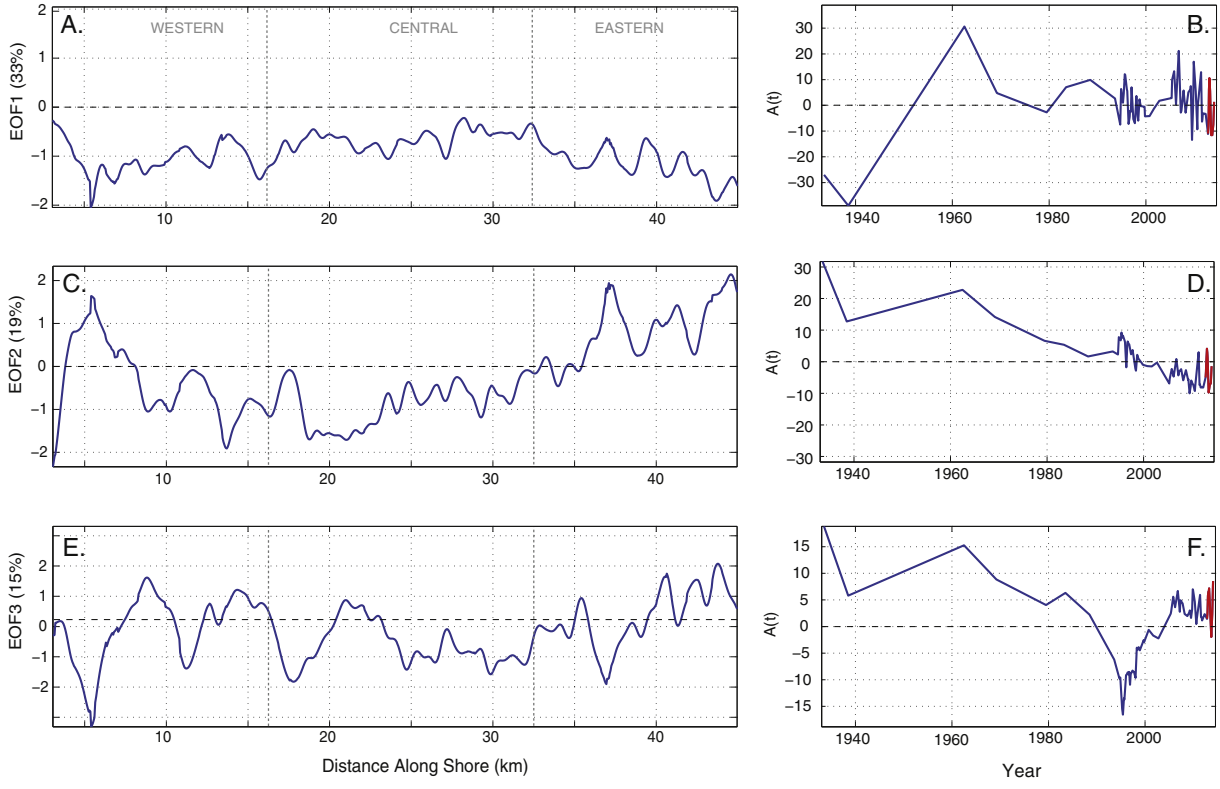

Fig. 4. Lower order eigenfunctions which represent alongshore variability and amplitudes of the temporal coefficients for the mean-removed shoreline positions (1933–2014). The eigenfunctions are shown in the left column (A, C and E) and the amplitudes in the right-hand column (B, D and F). The spatial distribution of the eigenfunctions can be visually correlated to the 3 geologic zones shown in this figure and in Fig. 1. The portion of the dataset that includes Hurricane Sandy response and recovery is shown in red in the plots of the amplitude associated with each EOF mode. Note that the y-axes scale of EOF3 is different from EOF1 and EOF2 for visualization purposes.

observed on the western half of the island. The time-scale of change is much longer than individual storms (EOF 1) and is shorter than the long-term trend (EOF2).

4.3. Wave record analysis

The results of the historical wave analysis is provided in Table 2 and shown in Fig. 5a–d, along with the first 3 temporal EOF coefficients (Fig. 5e). From 1980 to 2015, the average wave height was 1.08 m and the wave period was 7.06 s. The time series shows no apparent long term trend in significant wave height (H_s) or mean wave period (T_m). There is a significant trend in the wave direction (α_w) that indicates a slight (~3°) northward rotation after 1995 (Table 2).

4.4. Storm response

In order to examine shoreline response to known storm events in the more recent, densely sampled time period, including the response and recovery to Hurricane Sandy in 2012, we isolate the more recent portion of the long-term time series, 1980–2014, from the data used to produce Fig. 4 (Fig. 6). The spatial eigenfunctions in Figs. 4 and 6 are the same for reference. Known, individual large storms of the 2004–2014 time period are identified in all three of the EOF amplitude time series (Fig. 6b, d and f). In all modes, large storms result in similar magnitude increases in amplitude. This includes the response from Hurricane Sandy, which was in comparison a far larger storm based on wave height and period than the other notable storms of the 2004–2014 record. One exception to the consistent storm response characteristic is the large negative excursion in the amplitude of EOF3 in the period from 1990 to 2004.

5. Discussion

Long-term time series of shoreline change provide an ideal dataset to understand the relative importance of coastal change drivers on barrier island evolution. Our analysis of the long-term time series at Fire Island indicates that the behavior and evolution of the barrier island, as represented by multi-temporal shoreline positions and long-term trend, is controlled by a combination of resolvable external and internal factors. The external factors are hydrodynamic processes associated with storms and the internal factors are linked to the geology of the coastal system in the form of variations in alongshore sediment availability and morphology (bathymetric variability and slope).

5.1. Hydrodynamic process and response

Our analysis indicates that shoreline variability that is coherent at the largest spatial scale (EOF1) is the most-rapidly changing, with fluctuations that are not usually resolved by the temporal sample rate. While the EOF approach does not inherently identify patterns of variability that represent different physical processes, the spatial coherence of EOF1 remains high across the entire study domain (with the exception of the very western portion, which is known to be a migrating spit). Therefore, the EOF 1 characteristics are interpreted to identify a physical process (e.g., rapid, spatially coherent storm response and recovery), rather than simply breaking down a noisy signal, for which EOF1 would be expected to explain the most variance in the central portion of the spatial domain (Merrifield and Guza, 1990) and progressively less variance towards the domain boundaries.

There is also distinct variability that is manifested in shoreline orientation (EOF2) and is a large spatial-scale phenomenon that changes over the longest times scales (century). This trend could be driven oceanographically, e.g., as a response to the subtle trend in wave angle, or it could be a differential response controlled by the different geologic constraints present along the island. Finally, shorter-length scale rhythmic features (EOF3) respond on intermediate timescales (decades). We note that EOF analysis effectively separates the long-term and short-term signals (e.g., EOF 1 and 2) from a dataset with variable sampling in time. EOF analysis is particularly appropriate for this irregularly sampled dataset, as it finds spatial patterns that represent

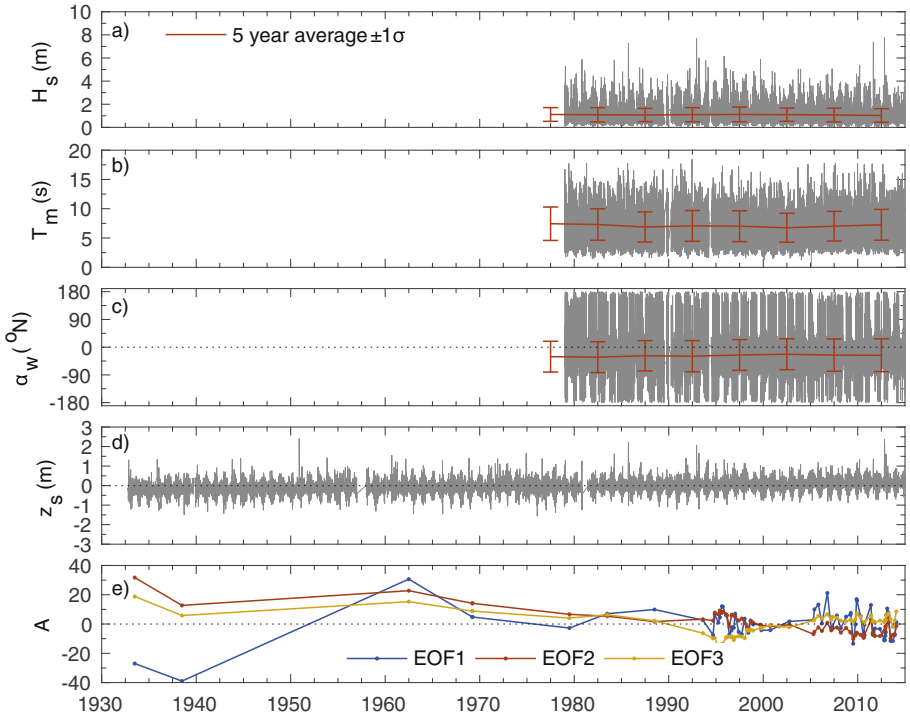

Fig. 5. Time series of a) significant wave height (H_s, m); b) mean wave period (T_m, s); c) mean direction of wave propagation (α_w, degrees from north); d) surge (z_s, m); and e) temporal EOF coefficient (A). The filtered signal (red line) is a 90 day moving average in a–c and a 1 year moving average in d.

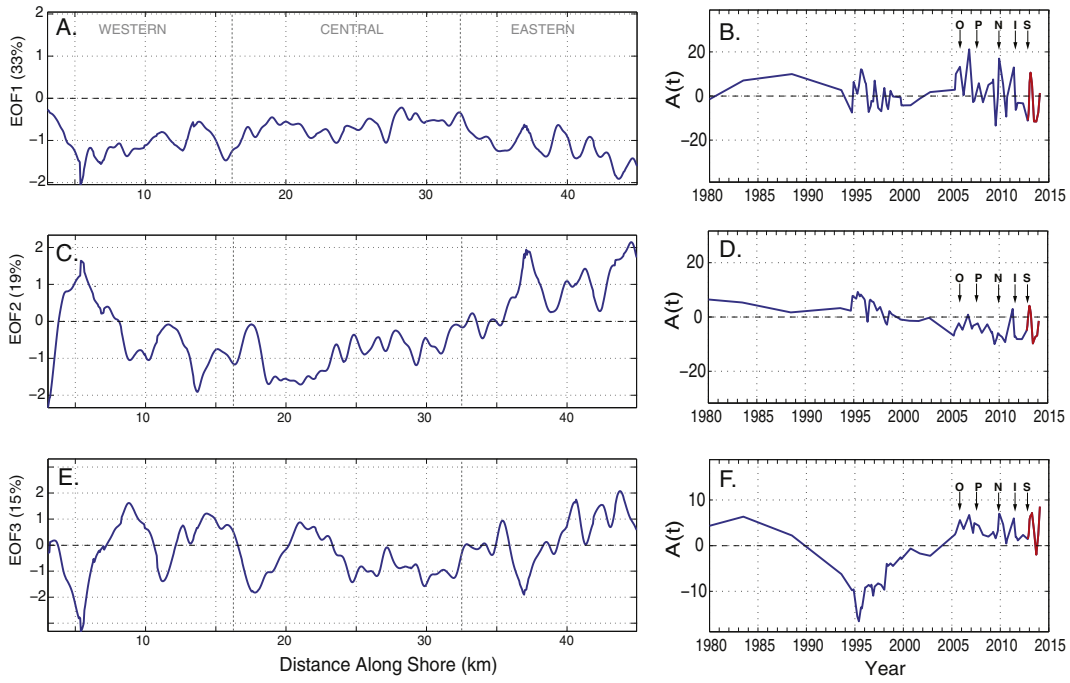

Fig. 6. Lower order eigenfunctions which represent alongshore variability and amplitudes of the temporal coefficients. The eigenfunctions are shown in the left column (A, C and E) and the amplitudes in the right column (B, D and F). The spatial distribution of the eigenfunctions can be visually correlated to the 3 geologic zones shown in this figure and in Fig. 1. The amplitude data are subsetted from Fig. 5 in order to resolve the more recent time period from 1980 to 2014. The temporal coefficients are the same as those shown in Fig. 5. The portion of the dataset that includes Hurricane Sandy response and recovery is shown in red in the plots of the amplitude associated with each EOF mode. Storms of note over the past decade are indicated by the arrows and letters: O = Oct. 2005 nor'easter; P = 2007 Patriot's Day nor'easter; N = 2009 Nor'Ida storm; I = 2011 Hurricane Irene; S = 2012 Hurricane Sandy. Note that the y-axes scale of EOF3 is different from EOF1 and EOF2 for visualization.

shoreline variability over the entire sample period and spatial extent. Alternatively, focusing the analysis on only the more recent, more frequently sampled period leads to mixing of the long-term and short-term signals and results in poor separation of trends. To test this, we repeated the analysis on the period 1980 to present and found two dominant modes: the first was essentially the same as our original EOF1 with a slight trend added to it and the second was similar to EOF3. We also performed a complex EOF analysis (e.g., Merrifield and Guza, 1990) which identified a dominant mode with nearly constant spatial phase (no alongshore propagation), and rapid variation in temporal phase (a standing wave consistent with shoreline erosion and deposition at short time scales).

While EOF1 is coherent across the much of the analysis domain, there are short-scale variations in its spatial pattern. The roll-off from a spatial autocorrelation of the amplitudes of the spatial eigenfunctions indicates that the shorter features have length scales less than about 1 km. These are superimposed on the large-scale structure (Fig. 4A), which is visually apparent in the time series array (Fig. 2). The oscillatory pattern of high variability with spatially alternating retreat and advancement is indicative of storm-related response and recovery of the beach, similar to reversing hotspots observed by List et al. (2006) and modeled by Valvo et al. (2006). In this response mode, storm waves reorganize sediment along the beach face resulting in distinct ~1 km cells where the shoreline either retreats or progrades. Lower energy waves gradually straighten the shoreline, thus reversing the storm shoreline configuration (Fig. 7A). Although our data are not able to resolve on the intra-seasonal scales that were resolved by List et al. (2006), our data do show patterns of persistence and reversal over longer time periods of years to decades (Fig. 2). One explanation for the oscillatory pattern in the shoreline record is that variations in temporal sediment flux that produce longshore sand waves result in gradual shoreline advancement followed by retreat as packages of sand propagate alongshore (Hicks and Inman, 1987; Stive et al., 1990; Stive et al., 2002). However, there is little evidence of alongshore propagation of pulses of sediment at Fire Island (Fig. 2), in agreement with our CEOF analysis and findings by Gravens (1999), with the exception of the time period from approximately 1994 to 2002. The oscillations also appear abrupt (sub-year) based on the more recent time period (Figs. 4B and 6B), rather than a pattern of gradual (multi-year) retreat and advancement, as is described for propagating sand waves. Temporary reversals in the sign of the oscillations (retreated hotspots becoming advanced hotspots) are associated with major storm events, for example Nor'Ida in 2009, Hurricane Irene in 2011, and Hurricane Sandy 2012 (Fig. 6B). A return to a pre-storm state is indicative of recovery processes by which waves move sediment landward in the surfzone as wave energy returns to non-storm conditions. The geomorphic manifestation of this process is that the shoreline becomes more variable for a period (sub-year) following storm events as sand is mobilized and deposited, reorganizing to return to a pre-storm state.

The short spatial scale (<1 km) storm-related oscillations superimposed on the alongshore-uniform structure of EOF1 is well correlated to the spatial variability of the long-term linear regression (correlation coefficient is 0.75), indicating that there is coupling between the long-term shoreline trends (which we interpret to be controlled by the framework geology) and the short-term variations associated with storms.

The data analyzed in this study includes shorelines before and after Hurricane Sandy, allowing for investigation of how extreme storms resolve in the long-term record as well as compare to severe, but lesser storm events. Hurricane Sandy was a significant event at Fire Island in terms of overwash, island breaching and dune elevation changes (e.g. Hapke et al., 2013). However, our analysis indicates that the shoreline response from Sandy was not unique in magnitude or character than other recent large storms such as Nor'Ida (2009) and Hurricane Irene (2011). Each of these storms, as well as moderately large nor'easters in 2005 and 2007, caused rapid phase shifts that were short-lived (years) (Fig. 6B, D, and F). The short duration of the impact and the lack of temporal trend in EOF1 and 3, suggests that, in the short term,

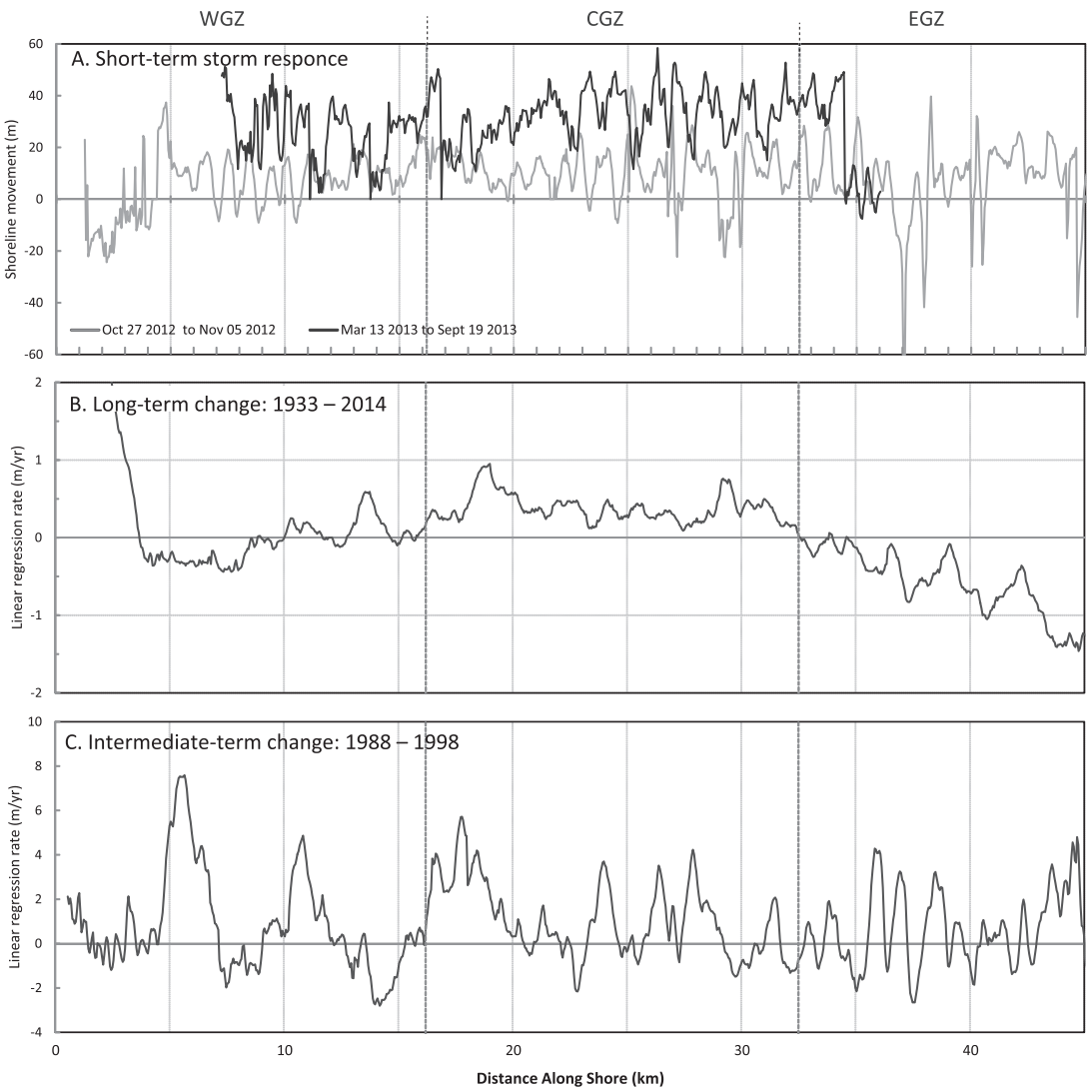

Fig. 7. Geomorphic responses associated with EOF modes: A) short-term change represented by net shoreline movement measured for Hurricane Sandy (Oct. 27–Nov. 5, 2012) and a period of post-storm recovery (Mar. 13–Sept. 19, 2013) showing the geomorphic response with shoreline undulations of retreat and advance on the order of 1 km length-scale associated with the variance in EOF1; B) long-term rates of shoreline change (see also, Fig. 3) indicating differential geomorphic behavior of the island which is similar in character to the spatial variance in EOF2; C) shoreline change rates for the period from 1988 to 1998, in which the intermediate time-scale of shoreline variance demonstrated in EOF3 is shown in the shoreline behavior.

the island is maintaining a relatively stable configuration. The beginning of a marked, long duration (15 year) negative excursion of the temporal amplitude in EOF3 coincides with major nor'easters of the early 1990s that severely impacted Fire Island. A similar response might be expected from a storm with the magnitude of Hurricane Sandy given the large amount of cross-shore transport that occurred during the storm, but there is no evidence for this in the shoreline variance. It appears that the frequency and duration of the early 1990s storms altered the state of the preferred shoreline configuration (Figs. 2 and 6C), possibly due to lack of sufficient recovery time between major events. However, the winter following Sandy had a series of large nor'easter events – seven storms with offshore significant wave heights of greater than four meters (Hapke et al., 2013). The lack of anomalous signal in shoreline variance from Hurricane Sandy (as compared to the 1990s nor'easters) is likely due to the substantial amount of sediment that was mobilized during the storm. Although there was significant transport of material to the interior and back-bay portions of the island (Hapke et al., 2013), large volumes were transported from the beach and dunes to upper shoreface and were available for the short-term recovery of the shoreline (Nelson and Hapke, 2015). The results suggest that extreme nor'easter storms or a period of large storms in succession have the potential to disrupt long-term trends more significantly and for longer time periods than isolated tropical storms at Fire Island (Figs. 2 and 6C).

The lack of a temporal trend in the amplitude of EOF1, especially in the more recent period from 1980 to 2014 (Figs. 4D and 6D), suggests that impacts of sea-level rise, effects of island reorientation, and nourishment activities have not yet influenced the magnitude of storm impacts at Fire Island. This supports other findings in our analysis that the Fire Island barrier system is relatively resilient.

5.2. Geologic processes and evolution

EOF2 has a distinct along-island spatial variability that consists of changes of sign in the different island regions (WGZ, CGZ, EGZ) as well as short-scale spatial variability that is broadly distributed over length scales shorter than 5 km. Alongshore variability in the long-term shoreline change has been related to the geology in the form variations in slope of the beach system (Lentz et al., 2013) and alongshore sediment availability and bathymetric features on the inner continental shelf (Hapke et al., 2010; Schwab et al., 2000, 2013). These physical variations have been established as representing framework geology

variations and as thus defined can influence the processes that shape the barrier island. The spatial pattern of EOF2 is strongly correlated to the long-term linear regression of shoreline change (correlation coefficient is 0.92), as expected since the temporal response of this mode is dominated by a long-term trend (Fig. 4D). We contend that the strong correlation between EOF2 and the long-term shoreline change pattern statistically demonstrates the influence of geologic processes, or processes influenced by framework geology, on barrier island evolution because the EOF analysis not only produces the same patterns but shows that they are spatially coherent over very long length scales. Similar to findings of Lazarus and Murray (2011) along the Outer Banks of North Carolina, when the smaller length-scale, rapidly changing shoreline patterns are removed (EOF1), the patterns of geologically-influenced long-term change are exposed. The long-term shoreline change rates (Figs. 3 and 7B) provide evidence that the geomorphic expression of the island results from persistent landward movement of the EGZ, seaward movement of the CGZ, and landward-seaward oscillation in the WGZ.

Wave fields can be modified by variable shelf morphology (O'Reilly and Guza, 1993), such as the paleo-outwash deposit in the CGZ or the sand ridge field in the CGZ and WGZ at Fire Island, resulting in wave refraction that alters the hydrodynamics closer to the shoreline. Additionally, ridge fields have been found to dissipate wave energy associated with storms along the Dutch coast (van de Meene et al., 1996). Similar deposits exist adjacent to barrier islands along the U.S. eastern seaboard (Duane et al., 1972; McBride and Moslow, 1991; Schwab et al., 2000) and elsewhere, and the effects of these and similar features on barrier island evolution are observed not only at Fire Island, but as demonstrated by Houser et al. (2008) and Houser (2012) in the Gulf of Mexico, and McNinch (2004) and Schupp et al. (2006) along the Outer Banks of North Carolina.

It is expected that the steeper and deeper morphology of the inner continental shelf off the EGZ at Fire Island (Schwab et al., 2013) results in higher wave energy reaching this portion of the coast (Davis, 1994) as compared to the CGZ and WGZ, increasing both cross-shore and alongshore sediment fluxes. The steeper slope maintained by the beach system and higher cross-shore sediment fluxes during storms (Lentz et al., 2013) is evidence of higher wave energy along the EGZ. The steeper and deeper morphology in EGZ is a function of the variable framework geology affecting evolutionary processes.

In addition, the volume of modern sand on the inner continental shelf along Fire Island, a function of sediment thickness, is highly variable and the region offshore of the EGZ is largely devoid of modern sediment (Fig. 1; Schwab et al., 2014). In contrast, the CGZ and WGZ have an abundance of modern sediment. Schwab et al. (2014) provide evidence that the modern sediment distribution extends into the lower shoreface. It is reasonable to assume that the relative distribution of sand in the shoreface is a function of sand availability on the inner shelf and in turn the distribution of sand in the littoral system a function of sand availability in the shoreface. The volume and distribution of modern sand are thus a result of the framework geology. Material transported inland as overwash and breaching during large storms is lost to the littoral system. To maintain the shoreline position, sediment from the shoreface would be required to replenish the lost littoral sediment, a process that is necessary to achieve the observed long-term maintenance of the barrier island.

5.3. Additional process controls

The final mode that we retain in the analysis, EOF3, consists of broad oscillations in the WGZ and the western portion of the CGZ (length scale of 6.3 km, based on spatial autocorrelation) and describes high amplitude, large excursions along the length of Fire Island (Fig. 4E). The spatial variations are only weakly correlated to the long-term linear regression (correlation coefficient is 0.34), indicating that they are attributable to a process that differs from the one driving long-term retreat and advancement of the shoreline identified in EOF2. The largest wavelengths occur on the western half of the island and the retreat and advancement excursions have a characteristic wave length that is similar in length-scale, but generally out of phase, to the excursions in EOF2. The locations of focused shoreline retreat and advancement are maintained over long periods of time with small amplitude increases that are storm-related (Figs. 2 and 4F).

It is unclear what processes are creating and maintaining the large-scale oscillations, which resembled a standing wave in both EOF2 and 3. Slight changes in the angle of wave approach can alter the alongshore sediment flux and produce irregularities in the shoreline that could be maintained if the wave direction persisted for some period of time (Ashton et al., 2001; Ashton and Murray, 2006). Excursions in the shoreline maintained by a persistent wave approach may become diffusive if the wave angle relative to the shoreline is reduced sufficiently. The wave analysis (Table 2 and Fig. 5) indicates that the wave angle relative to the shoreline at Fire Island has slightly increased, which would increase the tendency for shoreline excursions. The overall morphology of the island may not be persistently embayed because the processes creating the oscillations in EOF2 and 3 are out of phase and may act together like a progressive wave that somewhat resembles alongshore propagating sand waves. The geomorphic expression of EOF3 is demonstrated in Fig. 7C, which shows the decadal linear regression rates from 1988 to 1998, a subset of our time series. The patterns of shoreline change during this period clearly show large (~6 km length scale) positive shoreline excursions indicating zones of progradation adjacent to zones of retreat along the WGZ and the western portion of the CGZ, from 0 to 23 km alongshore. The length scale decreases to the east and there is no evidence of a sustained length scale of the retreat versus advanced cells.

The sign of the temporal coefficient of EOF3 remains the same over several decades (Fig. 4F), leading to the persistence of the zones of advanced and retreated shorelines, with the exception of a significant excursion that peaked in 1995. In the time period between 1990 and 1995, the zones reversed and their amplitudes increased rapidly. This major system reconfiguration is associated with the series of severe nor'easter storms that occurred in rapid succession in 1991, 1992, and 1993, and potentially forced an unstable state. Over a decadal time period following the early 1990s nor'easters, the amplitudes steadily decreased and for the most recent decade remain similar to pre-1990s magnitudes and sign (Fig. 6F). The eventual return to a pre-1990s behavior (Figs. 2 and 6F) after the storms of the early 1990's supports that there is a preferred configuration of the shoreline response, further demonstrating geological control and overall island stability.

5.4. Management implications

The separable and distinct behaviors which define shoreline morphodynamics and evolution at Fire Island have significance for both coastal management and for the development and refinement of predictive models. Management actions can benefit not only from the enhanced understanding of the along-island morphodynamics, but also through the recognition that specific locations along the coast have a preferred response which may aid in decisions to manage different sections of the island in different ways.

6. Conclusions

Our study of variance using empirical orthogonal function analysis of a long-term shoreline database demonstrates that the primary controls on shoreline response along a geologically-variable barrier island can be resolved on time scales ranging from storm events to decadal variations over a period of nearly one century.

Short-term storm response and recovery dominates the shoreline behavior on the largest spatial scales (along the entire barrier island). There is no conclusive indication of a trend through time in the storm response mode of the shoreline implying that the Fire Island barrier

shoreline is stable over decade to century scales. In support of this conclusion is the shoreline response to Hurricane Sandy in 2012, which was the largest storm on record for Fire Island but is not differentiable from a number of severe but lesser storms of the previous decade.

The analysis of the long time series also provides a quantitative approach to support that long-term shoreline evolution is controlled by the framework geology of the system represented by known variations in inner shelf bathymetry, beach-shoreface morphology, and long-term rates of shoreline change. The geologic processes that control long-term morphodynamics result in the ends of the island responding in opposite phase to the central portion; this behavior is not simply an artifact of the statistical methods approach since the long record of geomorphic change of the barrier island also supports a geological control. The differential evolution of the barrier, therefore, is a function of the geological history of the region even prior to the formation of the barrier itself.

An additional mode of variance in shoreline response reveals an intermediate-scale pattern that persists over both long and short-term time scales. Although speculative, we suggest that the pattern results from an unresolved combination of, or feedback between, storm processes and framework geology (bathymetric variability and sediment availability). The temporal record suggests there is a preferred configuration of shoreline response that can be periodically disrupted in association with major storms, but the deviations are not large and are short-lived (sub-year), supporting that the island is in a stable configuration. The exception to the stable configuration is the response associated with a period of frequent, severe nor'easters in the early 1990s; the recovery from this exceptionally stormy period took approximately a decade.

Acknowledgements

The data for this paper are available at the USGS National Assessment of Coastal Change Hazards Portal: http://marine.usgs.gov/coastalchangehazardsportal/ and from USGS Data Series 931 (http://pubs.usgs.gov/ds/0931/). Funding for this research was provided by the USGS Coastal and Marine Geology Program and the USGS Natural Resource Preservation Program. Owen Brenner provided field support and assisted with data acquisition and graphics. We would like to thank Jeff List and Jennifer Miselis (USGS) for fruitful discussions that enhanced the paper, Amy Farris (USGS) for assistance with code development and deriving shorelines. BJ Reynolds, Barry Irwin (USGS) and Jordan Rafael (NPS) provided valuable field assistance.

References

Ashton, A.D., Murray, A.B., 2006. High-angle wave instability and emergent shoreline shapes: 1. Modeling of sand waves, flying spits, and capes. J. Geophys. Res. 111, F04011. http://dx.doi.org/10.1029/2005JF000422.

Ashton, A.D., Murray, A.B., Arnoult, O., 2001. Formation of coastline features by large-scale instabilities induced by high-angle waves. Nature 414, 296–300. http://dx.doi.org/10.1038/35104541.

Belknap, D.F., Kraft, J.C., 1985. Influence of antecedent geology on stratigraphic preservation potential and evolution of Delaware's barrier systems. Mar. Geol. 63, 235–262. http://dx.doi.org/10.1016/0025-3227(85)90085-4.

Birchler, J.J., Dalyander, P.S., Stockdon, H.F., Doran, K.S., 2015. National assessment of nor'easter-induced coastal erosion hazards—mid- and northeast Atlantic coast. U.S. Geological Survey Open-File Report 2015-1154 http://dx.doi.org/10.3133/ofr20151154.

Davis, R.E., 1976. Predictability of sea surface temperature and sea level pressure anomalies over the North Pacific Ocean. J. Phys. Oceanogr. 6, 249–266. http://dx.doi.org/10.1175/1520-0485(1976)006%3C0249:POSSTA%3E2.0.CO;2.

Davis, R.A., 1994. Barrier island systems – a geologic overview. In: Davis, R.A. (Ed.), Geology of Holocene Barrier Islands. Springer-Verlag, pp. 1–48.

Dick, J.E., Dalrymple, R.A., 1984. Coastal changes at Bethany Beach, Delaware. Proceedings of the 19th International Conference on Coastal Engineering. ASCE Publishing, New York, NY, pp. 1650–1667.

Duane, D.B., Field, M.E., Meisburger, E.P., Swift, D.J.P., Williams, S.J., 1972. Linear shoals on the Atlantic inner shelf, Florida to Long Island. In: Swift, D.J.P., Duane, D.B., Pilkey, O.H. (Eds.), Shelf Sediment Transport. Dowden, Hutchinson, and Ross, pp. 447–449.

Garrett, C.J.R., Toulany, B., 1981. Variability of the flow through the Strait of Belle Isle. J. Mar. Res. 39, 163–189.

Gravens, M.B., 1999. Periodic shoreline morphology, Fire Island, New York. In: Kraus, N.C., McDougal, W.G. (Eds.), Coastal Sediments, '99. American Society of Civil Engineers, Reston, VA, pp. 1613–1626.

Hapke, C.J., Lentz, E.E., Gayes, P.T., McCoy, C.A., Hehre, R.E., Schwab, W.C., Williams, S.J., 2010. A review of sediment budget imbalances along Fire Island, New York: can nearshore geologic framework and patterns of shoreline change explain the deficit? J. Coast. Res. 26, 510–522. http://dx.doi.org/10.2112/08-1140.1.

Hapke, C.J., Himmelstoss, E.A., Kratzmann, M., List, J., Thieler, E.R., 2011a. National assessment of shoreline change: historical shoreline change along the New England and Mid-Atlantic coasts. U.S. Geological Survey Open-file Report 2010-1118 http://pubs.usgs.gov/of/2010/1118/.

Hapke, C.J., Schwab, W.C., Gayes, P.T., McCoy, C., Viso, R., Lentz, E.E., List, J., 2011b. Inner shelf morphologic controls on the morphodynamics of the beach and bar system, Fire Island, New York. In: Rosati, J.D., Wang, P., Roberts, T.M. (Eds.), Coastal Sediments '11. American Society of Civil Engineers, Reston, VA, pp. 1034–1047.

Hapke, C.J., Brenner, O., Hehre, R., Reynolds, B.J., 2013. Coastal change from Hurricane Sandy and the 2012–13 winter storm season: Fire Island, New York. U.S. Geological Survey Open-File Report 2013-1231 http://pubs.usgs.gov/of/2013/1231/.

Henderson, R.H., Hapke, C.J., Brenner, O.T., Reynolds, B.J., 2015. Hurricane Sandy beach response and recovery at Fire Island, New York: Shoreline and beach profile data, October 2012 to October 2014. U.S. Geological Survey Data Series 931 http://dx.doi.org/10.3133/ds931.

Hicks, D.M., Inman, D.L., 1987. Sand dispersion from an ephemeral delta on the Central California coast. Mar. Geol. 77, 305–318. http://dx.doi.org/10.1016/0025-3227(87)90119-8.

Himmelstoss, E.A., Kratzmann, M., Hapke, C.J., Thieler, E.R., List, J., 2010. The national assessment of shoreline change: a GIS compilation of vector shorelines and associated shoreline change data for the New England and Mid-Atlantic coasts. U.S. Geological Survey Open-File Report 2010-1119 http://pubs.usgs.gov/of/2010/1119.

Houser, C., 2012. Feedback between ridge and swale bathymetry and barrier island storm response and transgression. Geomorphology 173, 1–16. http://dx.doi.org/10.1016/j.geomorph.2012.05.021.

Houser, C., Hapke, C., Hamilton, S., 2008. Controls on coastal dune morphology, shoreline erosion, and barrier island response to extreme storms. Geomorphology 100, 223–240. http://dx.doi.org/10.1016/j.geomorph.2007.12.007.

Lazarus, E., Murray, A.B., 2011. An integrated hypothesis for regional patterns of shoreline change along the Northern North Carolina Outer Banks, USA. Mar. Geol. 281, 85–90. http://dx.doi.org/10.1016/j.margeo.2011.02.002.

Leatherman, S.P., 1985. Geomorphic and stratigraphic analyses of Fire Island, New York. Mar. Geol. 63, 173–195. http://dx.doi.org/10.1016/0025-3227(85)90083-0.

Lentz, E.E., Hapke, C., 2011. Geologic framework influences on the geomorphology of an anthropogenically modified barrier island: assessment of dune/beach changes at Fire Island, New York. Geomorphology 126, 82–96. http://dx.doi.org/10.1016/j.geomorph.2010.10.032.

Lentz, E.E., Hapke, C.J., Stockdon, H.F., Hehre, R.E., 2013. Improving understanding of near-term barrier island evolution through multi-decadal assessment of morphologic change. Mar. Geol. 337, 125–139. http://dx.doi.org/10.1016/j.margeo.2013.02.004.

Lippmann, T.C., Holman, R.A., 1990. The spatial and temporal variability of sand bar morphology. J. Geophys. Res. 95 (C7), 11575–11590. http://dx.doi.org/10.1029/JC095iC07p11575.

List, J.H., Farris, A., Sullivan, C., 2006. Reversing storm hotspots on sandy beaches: spatial and temporal characteristics. Mar. Geol. 226 (3–4), 261–279. http://dx.doi.org/10.1016/j.margeo.2005.10.003.

McBride, R.A., Moslow, T.F., 1991. Origin, evolution, and distribution of shoreface sand ridges, Atlantic inner shelf, U.S.A. Mar. Geol. 97, 57–85. http://dx.doi.org/10.1016/0025-3227(91)90019-Z.

McNinch, J.E., 2004. Geologic control in the nearshore: shore-oblique sandbars and shoreline erosional hotspots, Mid-Atlantic Bight, USA. Mar. Geol. 211, 121–141. http://dx.doi.org/10.1016/j.margeo.2004.07.006.

Merrifield, M.A., Guza, R.T., 1990. Detecting propagating signals with complex empirical orthogonal functions: a cautionary note. J. Phys. Oceanogr. 20, 1628–1633. http://dx.doi.org/10.1175/1520-0485(1990)020<1628:DPSWCE>2.0.CO;2.

Miller, J.K., Dean, R.G., 2007. Shoreline variability via empirical orthogonal function analysis: part I temporal and spatial characteristics. Coast. Eng. 54, 111–113. http://dx.doi.org/10.1016/j.coastaleng.2006.08.013.

Miselis, J.L., McNinch, J.E., 2006. Calculating shoreline erosion potential using nearshore stratigraphy and sediment volume: Outer Banks, North Carolina. J. Geophys. Res. 111, F02019. http://dx.doi.org/10.1029/2005JF000389.

Morton, R.A., Clifton, H.E., Buster, N.A., Peterson, R.L., Gelfenbaum, G., 2007. Forcing of large-scale cycles of coastal change at the entrance to Willapa Bay, Washington. Mar. Geol. 246, 24–41. http://dx.doi.org/10.1016/j.margeo.2007.07.008.

Munoz-Perez, J.J., Medina, R., Tejedor, B., 2001. Evolution of longshore beach contour lines determined by the EOF method. Sci. Mar. 65 (4), 393–402.

Nelson, T.R., Hapke, C.J., 2015. Shoreface response and recovery to Hurricane Sandy: Fire Island, NY. In: Rosati, J.D., Wang, P., Gelfenbaum, G., Guza, R., Hanson, H., Ruggiero, P. (Eds.), Coastal Sediments '15. American Society of Civil Engineers, Reston, VA, pp. 1034–1047 http://dx.doi.org/10.1142/9789814689977_0012.

NOAA, 2014. National Data Buoy Center. http://www.ndbc.noaa.gov.

O'Reilly, W.C., Guza, R.T., 1993. A comparison of two spectral wave models in the Southern California Bight. Coast. Eng. 19 (3), 263–282. http://dx.doi.org/10.1016/0378-3839(93)90032-4.

Plant, N.G., Holman, R.A., Freilich, M.H., Birkemeier, W.A., 1999. A simple model for interannual sandbar behavior. Journal of Geophysical Research-Oceans 104 (C7), 15755–15776. http://dx.doi.org/10.1029/1999JC900112.

Plant, N.G., Holland, K.T., Puleo, J.A., 2002. Analysis of the scale of errors in nearshore bathymetric data. Mar. Geol. 191, 71–86. http://dx.doi.org/10.1016/S0025-3227(02)00497-8.

Riggs, S.R., Cleary, W.J., Snyder, S.W., 1995. Influence of inherited geologic framework on barrier shoreface morphology and dynamics. Mar. Geol. 126, 213–234. http://dx.doi.org/10.1016/0025-3227(95)00079-E.

Sallenger, A.H., 2000. Storm impact scale for Barrier Islands. J. Coast. Res. 16, 890–895http://coastal.er.usgs.gov/hurricanes/publications/jcr.html.

Schupp, C.A., McNinch, J.E., List, J.H., 2006. Nearshore shore-oblique bars, gravel outcrops, and their correlation to shoreline change. Mar. Geol. 233, 63–79. http://dx.doi.org/10.1016/j.margeo.2006.08.007.

Schwab, W.C., Thieler, E.R., Allen, J.R., Foster, D.S., Swift, B.A., Denny, J.F., 2000. Influence of inner-continental shelf geologic framework on the evolution and behavior of the barrier–island system between Fire Island Inlet and Shinnecock Inlet, Long Island, New York. J. Coast. Res. 16 (2), 408–422.

Schwab, W.C., Baldwin, W.E., Hapke, C.J., Lentz, E.E., Gayes, P.T., Denny, J.F., List, J.H., Warner, J.C., 2013. Geologic evidence for onshore sediment transport from the inner-continental shelf: Fire Island, New York. J. Coast. Res. 29 (3), 536–544. http://dx.doi.org/10.2112/JCOASTRES-D-12-00160.1.

Schwab, W.C., Denny, J.F., Baldwin, W.E., 2014. Maps showing bathymetry and modern sediment thickness on the inner continental shelf offshore of Fire Island, New York. U.S. Geological Survey Open-File Report 2014-1203 http://dx.doi.org/10.3133/ofr20141203.

Stive, M.J.F., Roelvink, D.J.A., de Vriend, H.J., 1990. Large-scale coastal evolution concept. 22nd International Conference on Coastal Engineering, Delft, The Netherlands, pp. 1962–1974.

Stive, M.J.F., Aaminkhof, S.G.J., Hamm, L., Hanson, H., Larson, M., Wijnberg, K.M., Nicholls, R.J., Capobianco, M., 2002. Variability of shore and shoreline evolution. Coast. Eng. 47, 211–235. http://dx.doi.org/10.1016/S0378-3839(02)00126-6.

Stockdon, H.F., Holman, R.A., Howd, P.A., Sallenger, A.H., 2006. Empirical parameterization of setup, swash, and runup. Coast. Eng. 53, 573–588. http://dx.doi.org/10.1016/j.coastaleng.2005.12.005.

Tătui, F., Vespremeanu-Stroe, A., Preoteasa, L., 2014. Alongshore variations in beach-dune system response to major storm events on the Danube Delta coast. J. Coast. Res. 693–699 http://dx.doi.org/10.2112/SI70-117.1 (Special Issue No. 70).

Taylor, J.R., 1997. An Introduction to Error Analysis: The Study of Uncertainties in Physical Measurement. University Science Books, Sausalito, CA, p. 327 http://dx.doi.org/10.1063/1.882103.

Thieler, E.R., Himmelstoss, E.A., Zichichi, J.L., Ergul, A., 2009. The Digital Shoreline Analysis System (DSAS) version 4.0-an ArcGIS extension for calculating shoreline change. Geological Survey Open-File Report 2008-1278 http://pubs.er.usgs.gov/publication/ofr20081278.

Valvo, L.M., Murray, A.B., Ashton, A., 2006. How does underlying geology affect coastline change? An initial modeling investigation. J. Geophys. Res. 111, F02025. http://dx.doi.org/10.1029/2005JF00340.

Van de Meene, J.W.H., Boersma, J.R., Terwindt, J.H.J., 1996. Sedimentary structures of combined flow deposits from the shoreface-connected ridges along the central Dutch coast. Mar. Geol. 131 (3–4), 151–175. http://dx.doi.org/10.1016/0025-3227(95)00074-7.

Viles, H.A., Goudie, A.S., 2003. Interannual, decadal and multidecadal scale climatic variability and geomorphology. Earth-Sci. Rev. 61, 105–131. http://dx.doi.org/10.1016/S0012-8252(02)00113-7.

Wijnberg, K.M., Terwindt, J.H.J., 1995. Extracting decadal morphologic behavior from high resolution, long-term bathymetric surveys along the Holland coast using eigenfunction analysis. Mar. Geol. 126, 301–330. http://dx.doi.org/10.1016/0025-3227(95)00084-C.

Winant, C.D., Inman, D.L., Nordstrom, C.E., 1975. Description of seasonal beach changes using empirical eigenfunctions. J. Geophys. Res. 80 (15), 1979–1986. http://dx.doi.org/10.1029/JC080i015p01979.

Woodroffe, C.D., 2003. Coasts: Form, Process and Evolution. Cambridge University Press, Cambridge, U.K., p. 623.

Wright, L.D., Short, A.D., 1984. Morphodynamic variability of surf zones and beaches: a synthesis. Mar. Geol. 56, 93–118. http://dx.doi.org/10.1016/0025-3227(84)90008-2.

Yates, M.L., Guza, R.T., O'Reilly, W.C., 2009. Equilibrium shoreline response: observations and modeling. Journal of Geophysical Research C: Oceans 114 (9). http://dx.doi.org/10.1029/2009JC005359.

Yates, M.L., Guza, R.T., O'Reilly, W.C., Hansen, J.E., Barnard, P.L., 2011. Equilibrium shoreline response of a high wave energy beach. J. Geophys. Res. 116, 1–13. http://dx.doi.org/10.1029/2010JC006681.